Available online at www.sciencedirect.com
ScienceDirect
Journal of Photochemistry and Photobiology A: Chemistry 184 (2006) 163–169
Journal of Photochemistry and Photobiology A:Chemistry
www.elsevier.com/locate/jphotochem

Synthesis, characterization, photocatalytic activity and dye-sensitized solar cell performance of nanorods/nanoparticles TiO_2 with mesoporous structure

Sorapong Pavasupree [a,b], Supachai Ngamsinlapasathian [a], Masafumi Nakajima [a], Yoshikazu Suzuki [a], Susumu Yoshikawa [a,*]

[a] *Institute of Advanced Energy, Kyoto University, Uji, Kyoto 611-0011, Japan*
[b] *Departments of Materials Metallurgical Engineering, Faculty of Engineering, Rajamangala University of Technology Thanyaburi, Klong 6, Pathumthani, 12110, Thailand*

Received 19 December 2005; received in revised form 9 March 2006; accepted 15 April 2006
Available online 27 April 2006

Abstract

Nanorods/nanoparticles TiO_2 with mesoporous structure were synthesized by hydrothermal method at 150 °C for 20 h. The samples characterized by XRD, SEM, TEM, SAED, HRTEM, and BET surface area. The nanorods had diameter about 10–20 nm and the lengths of 100–200 nm, the nanoparticles had diameter about 5–10 nm. The prepared material had average pore diameter about 7–12 nm. The BET surface area and pore volume of the sample are about 203 m^2/g and 0.655 cm^3/g, respectively. The nanorods/nanoparticles TiO_2 with mesoporous structure showed higher photocatalytic activity (I_3^- concentration) than the nanorods TiO_2, nanofibers TiO_2, mesoporous TiO_2, and commercial TiO_2 (ST-01, P-25, JRC-01, and JRC-03). The solar energy conversion efficiency (η) of the cell using nanorods/nanoparticles TiO_2 with mesoporous structure was about 7.12% with J_{sc} of 13.97 mA/cm^2, V_{oc} of 0.73 V, and f_f of 0.70; while η of the cell using P-25 reached 5.82% with J_{sc} of 12.74 mA/cm^2, V_{oc} of 0.704 V, and f_f of 0.649.

Keywords: Nanorods; Nanoparticles; Mesoporous; Anatase TiO_2; Photocatalytic activity; Dye-sensitized solar cell

1. Introduction

The synthesis and characterization of one-dimensional (1D) nanostructured materials (nanotubes, nanorods, and nanowires) have received considerable attention due to their unique properties and novel applications [1–4]. Much effort has concentrated on the important metal oxides, such as TiO_2, SnO_2, VO_2, and ZnO [1–9]. Among them, TiO_2 and TiO_2-derived materials are of importance for utilizing solar energy and environmental purification. TiO_2 has been widely used for various applications such as a semiconductor in dye-sensitized solar cell, water treatment materials, catalysts, gas sensors, and so on [10–27]. In our previous works, nanofibers TiO_2 were synthesized by hydrothermal and post heat-treatments from natural rutile sand, however, nanofibers TiO_2 had rather low surface area (10–20 m^2/g) [20,21]. The author's group preliminary reported that the nanowires/nanoparticles composite structure showed better photovoltaic conversion effect in dye-sensitized solar cell [22].

In this study, nanorods/nanoparticles TiO_2 with mesoporous structure (with much higher surface area, 203 m^2/g) has been synthesized, which shows high photocatalytic activity and high performance in dye-sensitized solar cell. The detail microstructure, photocatalytic, and photovoltaic properties will be reported.

2. Experimental

2.1. Synthesis

2.1.1. Nanorods/nanoparticles TiO_2 with mesoporous structure

Titanium(IV) butoxide (Aldrich) was mixed with the same mole of acetyacetone (ACA, Nacalai Tesque, Inc., Japan) to slowdown the hydrolysis and the condensation reactions [11–13]. Subsequently, distilled water 40 ml was added in the

* Corresponding author. Tel.: +81 774 38 3502; fax: +81 774 38 3508.
E-mail address: s-yoshi@iae.kyoto-u.ac.jp (S. Yoshikawa).

1010-6030/$ – see front matter © 2006 Elsevier B.V. All rights reserved.
doi:10.1016/j.jphotochem.2006.04.010

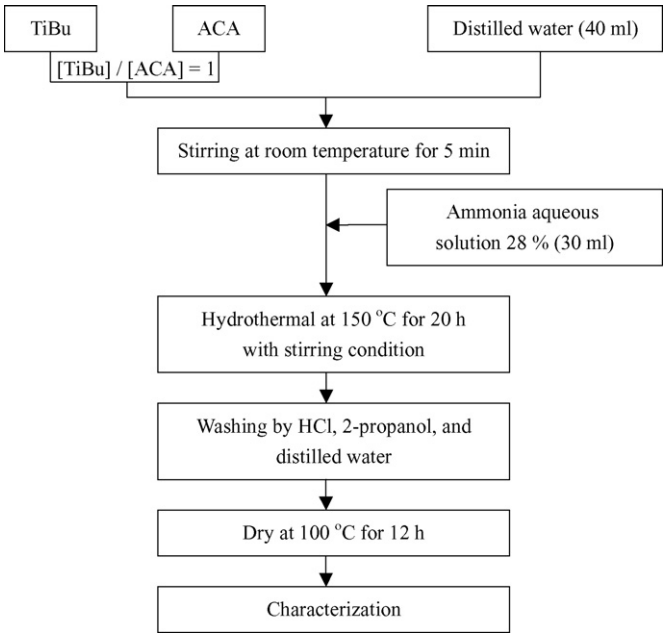

Fig. 1. Schematic representation for experimental procedure.

solution, and the solution was stirred at room temperature for 5 min. After kept stirring, ammonia aqueous solution 28% (Wako Co., Ltd., Japan) 30 ml was added in the solution, then the solution was put into a Teflon-lined stainless steel autoclave and heated at 150 °C for 20 h with stirring condition. After the autoclave was naturally cooled to room temperature, the obtained product was washed with HCl aqueous solution, 2-propanal and distilled water for several times, followed by drying at 100 °C for 12 h (Fig. 1). Using the similar procedure, nanorods TiO_2, nanofibers TiO_2, and mesoporous TiO_2 were also prepared for photocatalytic activity comparisons as follows.

2.1.2. Nanorods TiO_2

The nanorods TiO_2 were synthesized by using the same route of Section 2.1.1 but difference in the hydrothermal temperature at 170 °C for 72 h.

2.1.3. Nanofibers TiO_2

The nanofibers TiO_2 were synthesized by hydrothermal method (150 °C for 72 h) using natural rutile sand as the starting material and calcined at 700 °C for 4 h (prepared as refs. [20,21]).

2.1.4. Mesoporous TiO_2

The mesoporous TiO_2 were synthesized by surfactant-assisted sol–gel method at 80 °C for 5 days then calcined at 250 °C for 24 h (washed by 2-propanal) and 400 °C for 4 h (prepared as refs. [15–19]).

2.2. Characterization

The crystalline structure of the samples was evaluated by X-ray diffraction (XRD, RIGAKU RINT 2100). The microstructure of the prepared materials was analyzed by scanning electron microscopy (SEM, JEOL JSM-6500FE), transmission electron microscopy (TEM, JEOL JEM-200CX), and selected-area electron diffraction (SAED). The Brunauer–Emmett–Teller (BET) specific surface area was determined by the nitrogen adsorption (BEL Japan, BELSORP-18 Plus).

2.3. Photocatalytic activity measurement

The photocatalytic activity was measured through the formation rate of I_3^- due to the oxidation photo-reaction of I^- to I_2 in excess I^- conditions [11–13,19]. A reaction system was set up by adding 50 mg of a sample powder into 10 ml of 0.2 M of potassium iodide aqueous solution then stirred and irradiated with UV light (15 W, Vilber Lourmat VL-115L, with a maximum emission at about 365 nm) at room temperature. After the irradiation of 15, 30, 45, and 60 min, the suspension was withdrawn and centrifuged. After the clear supernatant was diluted 10 times, the concentration of liberated I_3^- ions was monitored by the absorbance at 288 nm, using an UV–vis spectrophotometer (Shimadzu UV 2450). The molar extinction coefficient was determined to be 4.0×10^4 (cm mol/l)$^{-1}$. No I_3^- formation was observed when the experiments were conducted in the dark or in the absence of the TiO_2 samples. For reference, four difference commercially available nanoparticles TiO_2 powders, ST-01 (Ishihara Sangyo Kaisha, Ltd., Japan), P-25 (Nippon Aerosil Co., Ltd., Japan), JRC-01, and JRC-03 (The Catalysis Society of Japan) were tested.

2.4. Dye-sensitized solar cell measurement

TiO_2 electrodes were prepared as follows: 1 g of TiO_2 powder was mixed with 0.1 ml of ACA, and was ground mechanically. During vigorous stirring, 5 ml of mixture of water and ethanol (1:1, in vol%) was added and 0.4 ml of polyoxethylene (10) octylphenyl ether (Triton X-100) was added to facilitate spreading of the paste on the substrate. The obtained colloidal paste was coated on fluorine-doped SnO_2 conducting glass (FTO, sheet resistance 15 Ω/□, Asahi glass Co., Ltd.) by squeegee technique. After coating, each layer was dried at room temperature and then annealed at 400 °C for 5 min. The coating process was repeated to obtain thick films. The resulting films were sintered at 450 °C for 2 h in air. Sintered TiO_2 electrodes were soaked in 0.3 mM of ruthenium(II) dye (known as N719, Solaronix) in a *t*-butanol/acetonitrile (1:1, in vol%) solution. The electrodes were washed with acetonitrile, dried, and immediately used for measuring photovoltaic properties. The electrolyte was composed of 0.6 M dimethylpropylimidazolium iodide, 0.1 M lithium iodide (LiI), 0.05 M iodide (I_2), and 0.5 M 4-*tert*-butylpyridine in acetonitrile.

The thickness of the TiO_2 films was measured with a Tencor Alpha-step Profiler. Photocurrent–voltage curve was measured under simulated solar light (CEP-2000, Bunkoh-Keiki, AM 1.5, 100 mW/cm^2). The light intensity of the illumination source was calibrated by using a standard silicon photodiode (BS520, Bunkoh-Keiki).

The amount of adsorbed dye was determined by desorbing the dye from the titania surface into a mixed solution of 0.1 M NaOH and ethanol (1:1, in volume fraction) and measuring its absorp-

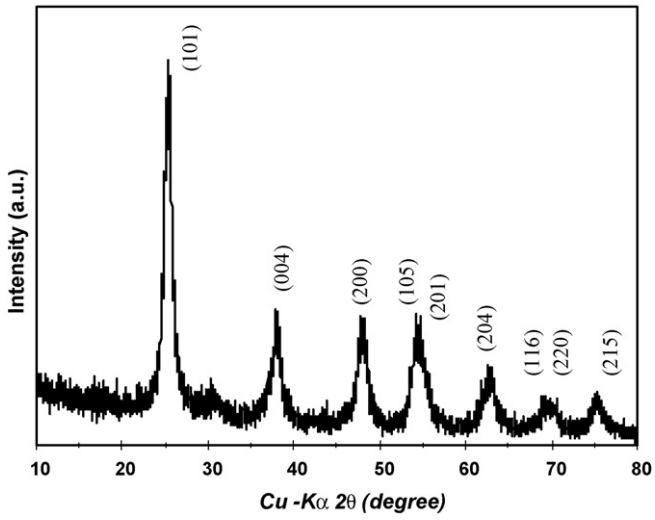

Fig. 2. X-ray diffraction pattern of the as-synthesized nanorods/nanoparticles TiO_2.

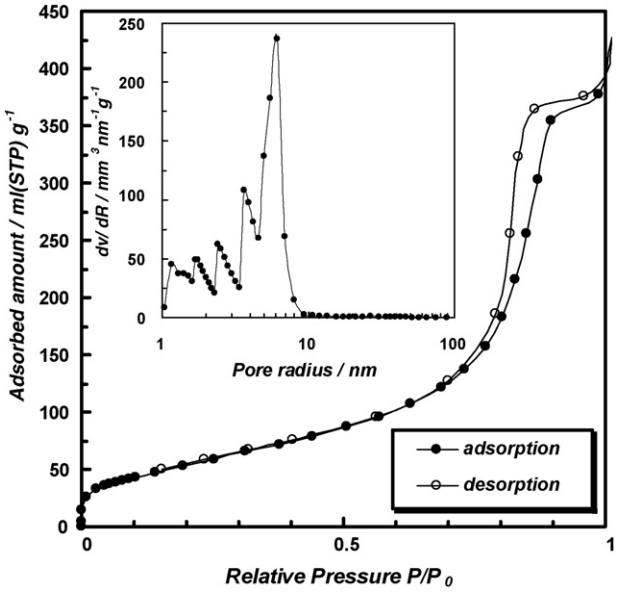

Fig. 3. Nitrogen adsorption isotherm pattern of the as-synthesized nanorods/nanoparticles TiO_2, and the pore size distribution of sample with pore diameter about 7–12 nm (inset).

tion spectrum. The concentration of adsorbed dye was analyzed by UV–vis spectrophotometer (UV-2450 SHIMADZU).

3. Results and discussion

3.1. Characterization results

Fig. 2 shows the X-ray diffraction pattern of the as-synthesized nanorods/nanoparticles TiO_2. The peaks were rather sharp, which indicated the obtained TiO_2 had relatively high crystallinity, and attributable to the anatase phase.

Fig. 3 gives the nitrogen adsorption isotherm and the pore size distribution of the as-synthesized nanorods/nanoparticles TiO_2. The isotherm shows a typical IUPAC type IV pattern with sharp inflection of nitrogen adsorbed volume at P/P_0 about 0.80 (type H_2 hysteresis loop), indicating the existence of mesopores. The pore size distribution of the sample, as shown in the inset of Fig. 3, showed that the nanorods/nanoparticles TiO_2 had average pore diameter about 7–12 nm. The BET surface area and pore volume of sample are about 203 m^2/g and 0.655 cm^3/g, respectively.

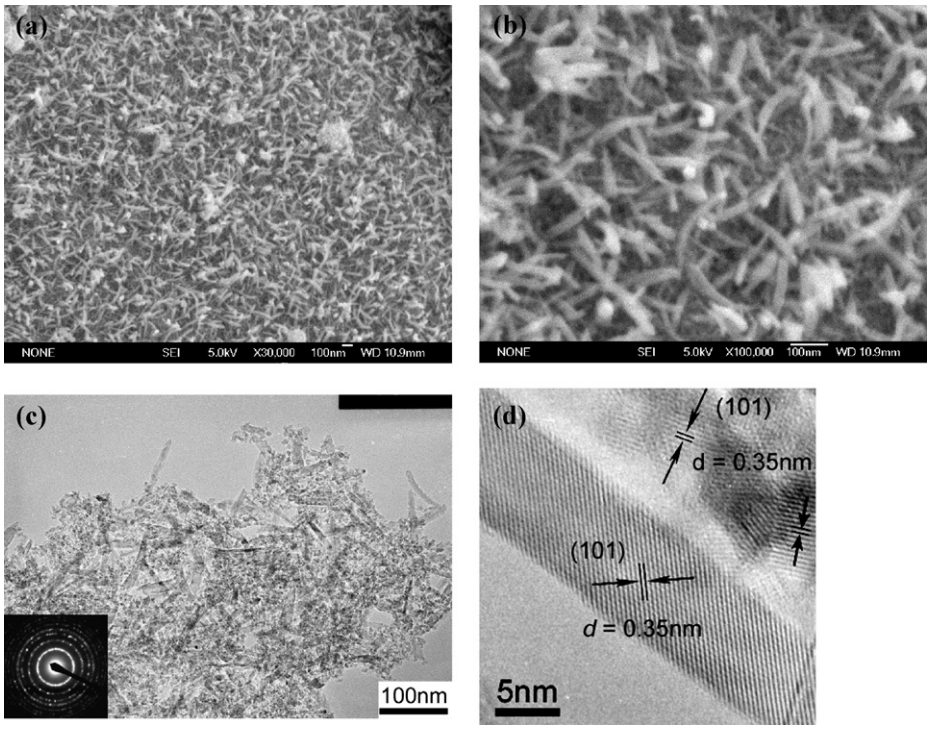

Fig. 4. (a and b) SEM, (c) TEM, SAED, and (d) HRTEM images of the as-synthesized nanorods/nanoparticles TiO_2.

Fig. 4(a and b) show SEM images of the as-synthesized nanorods/nanoparticles TiO_2, indicating the rods-like morphology. In addition, its TEM (Fig. 4(c)) clearly shows not only nanorods but also nanoparticles. The nanorods in the composite powder had diameter about 10–20 nm and the lengths of 100–200 nm, the nanoparticles had diameter about 5–10 nm. The electron diffraction pattern shown in the inset of Fig. 4(c) supported that the nanorods/nanoparticles composite was anatase-type TiO_2. The lattice fringes of the nanorods and the nanoparticles appearing in the image ($d = 0.35$ nm) also allowed for the identification of the anatase phase (Fig. 4(d)). HRTEM images of nanorods/nanoparticles with clear lattice fringes, again confirming its high crystallinity.

Figs. 5 and 6 show the summarized results (SEM, TEM, SAED, HRTEM, and BET surface area) of the prepared TiO_2 (nanorods TiO_2, nanofibers TiO_2, and mesoporous TiO_2), and commercial TiO_2 powders (ST-01, P-25, JRC-01, JRC-03).

The BET surface area of the nanorods TiO_2 (Fig. 5(a and b), anatase structure with diameter 60–80 nm and the lengths of 300–600 nm), the nanofibers TiO_2 (Fig. 5(c and d), anatase structure with diameter 20–100 nm and the lengths of several 10 μm), and mesoporous TiO_2 (Fig. 5(e and f), anatase structure with particles diameter 7–15 nm) were about 19, 10, and 80 m^2/g, respectively. The BET surface area of the commercial TiO_2, ST-01 (Fig. 6(a and b), anatase structure with particles diameter 4–5 nm), P-25 (Fig. 6(c and d), anatase 70% and rutile 30% structure with particles diameter 30–50 nm), JRC-01 (Fig. 6(e and f), anatase structure with particles diameter 15–30 nm), JRC-03 (Fig. 6(g and h), rutile structure with particles diameter 20–50 nm) were about 284, 56, 71, and 48 m^2/g, respectively.

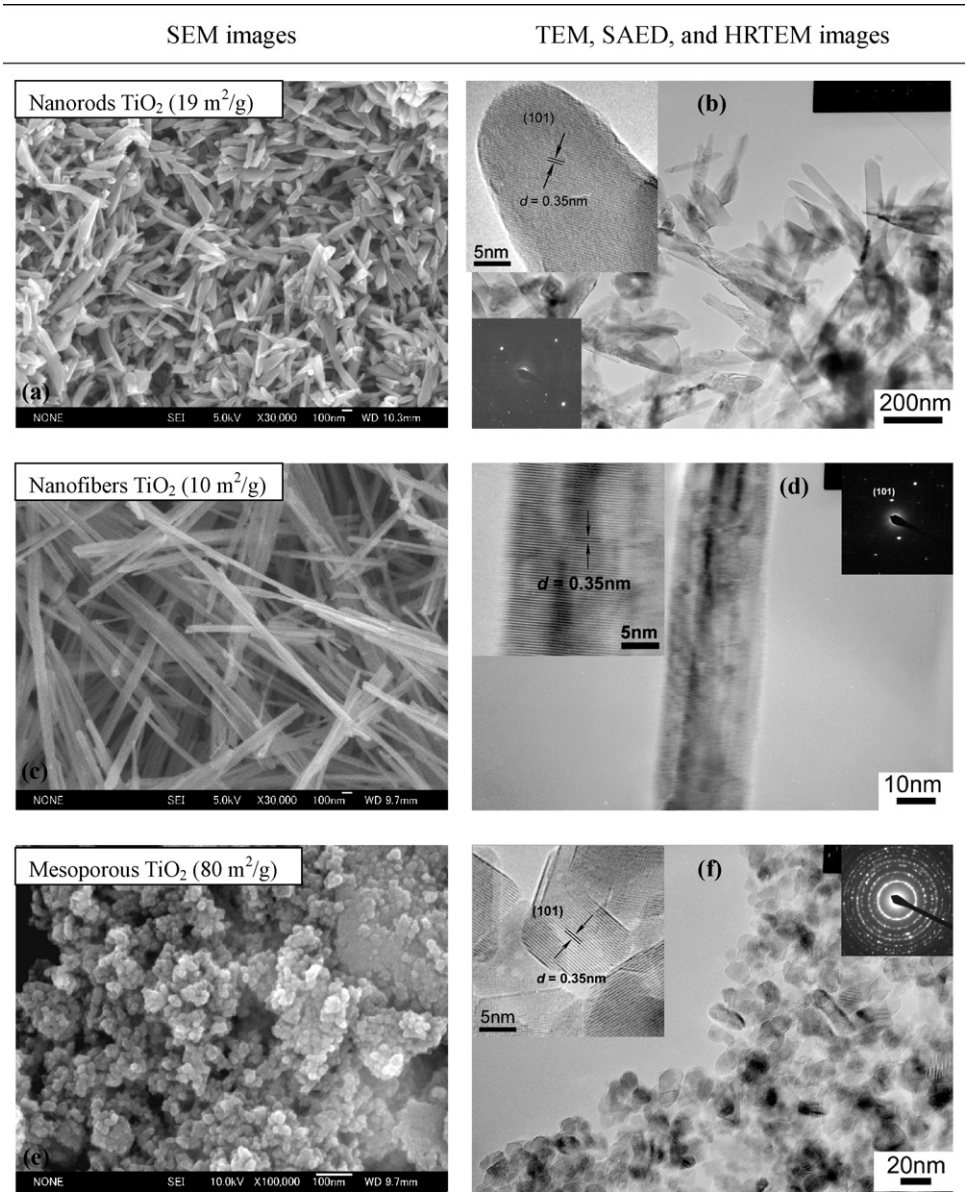

Fig. 5. SEM, TEM, SAED, HRTEM, and BET surface area results of the prepared TiO_2, (a and b) nanorods TiO_2 (prepared by hydrothermal at 170 °C, 72 h), (c and d) nanofibers TiO_2 (prepared as refs. [20,21]), and (e and f) mesoporous TiO_2 (prepared as refs. [15–19]).

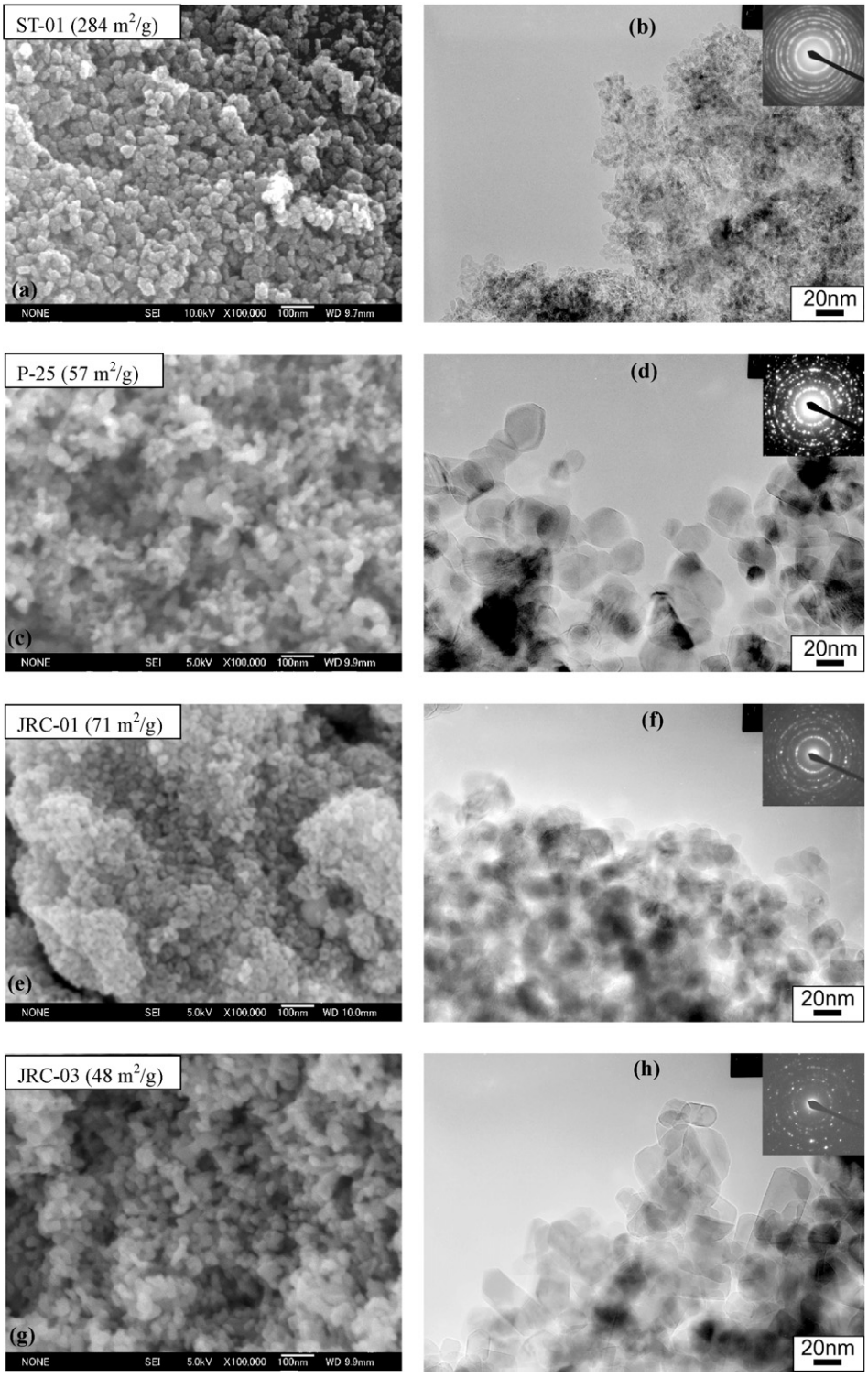

Fig. 6. SEM, TEM, SAED, HRTEM, and BET surface area results of the commercial TiO_2.

3.2. Photocatalytic activity results

The I_3^- concentration at 60 min of the irradiation period of the nanorods/nanoparticles TiO_2 were about 3.02×10^{-4} M (Fig. 7(a)), which is higher than that of other synthesized powders (nanorods TiO_2, nanofibers TiO_2, mesoporous TiO_2) and also that of four commercially available titania nanomaterials, ST-01, P-25, JRC-01, and JRC-03 which exhibit I_3^- concentration about 2.68×10^{-4}, 1.50×10^{-4}, 0.66×10^{-4}, and 0.25×10^{-4} M, respectively. The photocatalytic activity was almost proportional to the BET surface area (Fig. 7(b)), indicating that adsorption of I^- on titania surface was rate determining step in the initial stage of the reaction (before 15 min) [11–13]. In our previous works, it is obviously revealed that the introduction

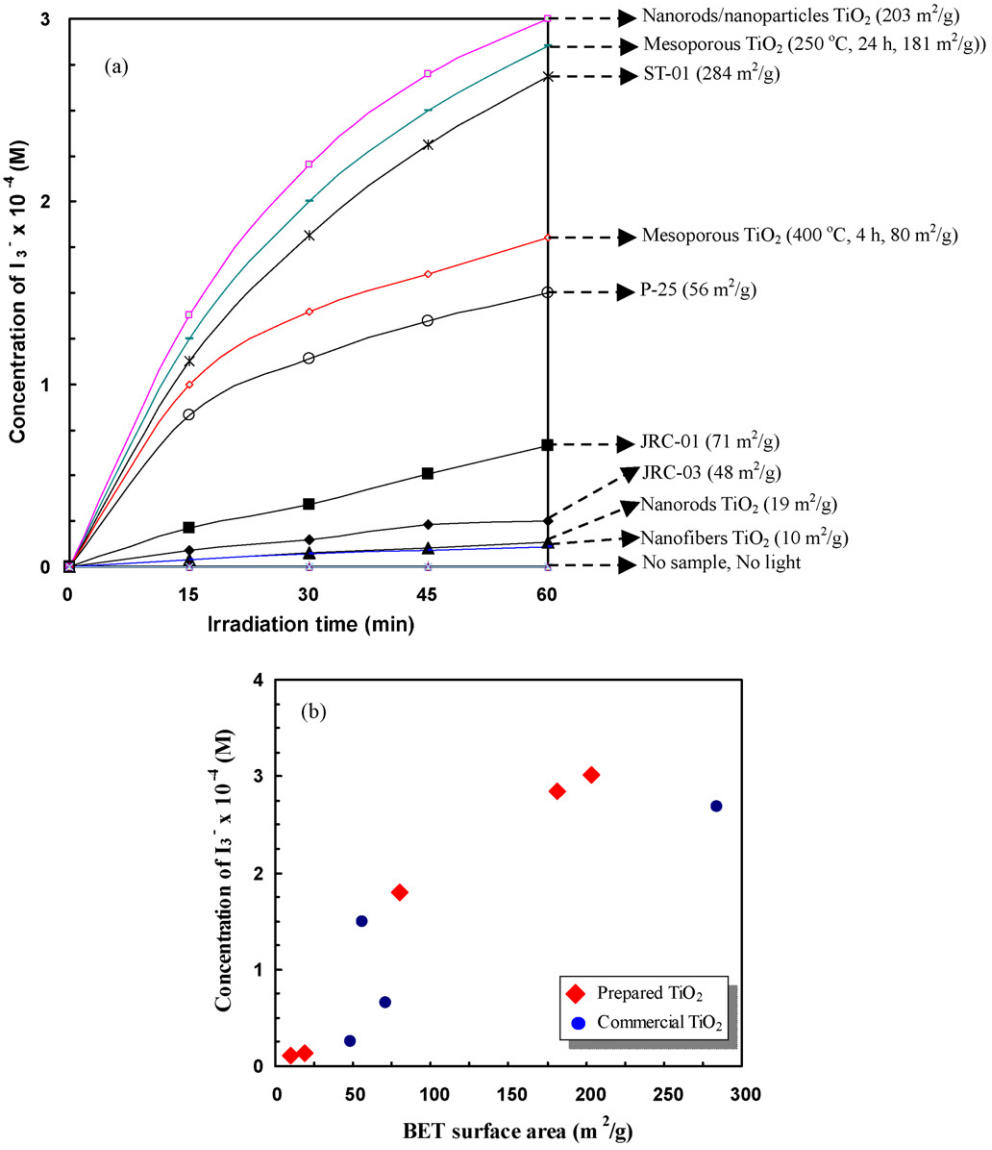

Fig. 7. (a) Photocatalytic activity (I_3^- concentration) of the nanorods/nanoparticles TiO_2 with mesoporous structure (prepared by this study), the mesoporous TiO_2 calcined at 250 °C for 24 h and 400 °C for 4 h (prepared as refs. [15–19]), the nanorods TiO_2 (prepared by this study), the nanofibers TiO_2 (prepared as refs. [20,21]), and commercial TiO_2 (ST-01, P-25, JRC-01, and JRC-03). (b) The comparison between I_3^- concentration–BET surface area of the prepared TiO_2 (nanorods/nanoparticles, mesoporous, nanorods, and nanofibers) and the commercial TiO_2 (ST-01, P-25, JRC-01, and JRC-03).

of mesopore into titania photocatalyst substantially improved the photocatalytic performance [17,19].

3.3. Dye-sensitized solar cell results

Fig. 8 shows comparison between photocurrent–voltage characteristics of the cell using nanorods/nanoparticles TiO_2 with mesoporous structure (thickness = 8.3 μm) and P-25 (thickness = 13.8 μm). The solar energy conversion efficiency of the cell using nanorods/nanoparticles TiO_2 with mesoporous structure was about 7.12% with J_{sc} of 13.97 mA/cm^2, V_{oc} of 0.73 V, and f_f of 0.70; while η of the cell using P-25 reached 5.82% with J_{sc} of 12.74 mA/cm^2, V_{oc} of 0.704 V, and f_f of 0.649. High current density and efficiency might be attributed to higher amount of adsorbed dye (11.44×10^{-8} mol/cm^2 for nanorods/nanoparticles TiO_2 and 5.68×10^{-8} mol/cm^2 for P-25), owing to larger surface area of the nanorods/nanoparticles TiO_2 (Table 1).

Table 1
BET surface area after calcined at 450 °C for 2 h and amount of adsorbed dye of nanorods/nanoparticles TiO_2 and P-25

Samples	BET surface area after calcined at 450 °C for 2 h (m^2/g)	Amount of adsorbed dye (mol/cm^2)
Nanorods/nanoparticles TiO_2	100	11.44×10^{-8}
P-25	54	5.68×10^{-8}

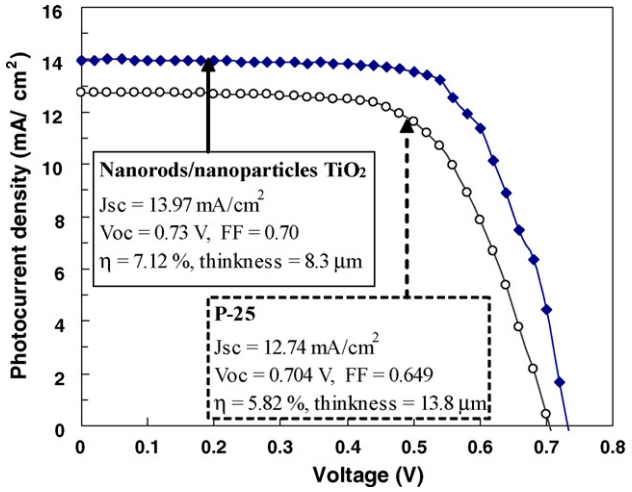

Fig. 8. The comparison between photocurrent–voltage characteristic of a typical dye sensitized solar cells fabricated by the nanorods/nanoparticles TiO_2 with mesoporous structure and P-25.

The nanorods/nanoparticles TiO_2 was found to be superior solar energy conversion efficiency to commercial nanoparticles P-25. The optimal thickness of this electrode should be further investigated. This material possesses high potential for further development in the application of dye-sensitized solar cells.

4. Conclusions

The results presented here demonstrated that the nanorods/nanoparticles TiO_2 with mesoporous structure could be synthesized by hydrothermal method at 150 °C for 20 h. The nanorods had diameter about 10–20 nm and the lengths of 100–200 nm, the nanoparticles had diameter about 5–10 nm. The prepared material had average pore diameter about 7–12 nm. The BET surface area and pore volume of sample are about 203 m^2/g and 0.655 cm^3/g, respectively. Nanorods/nanoparticles TiO_2 with mesoporous structure showed higher photocatalytic activity (I_3^- concentration) than the nanorods TiO_2, nanofibers TiO_2, mesoporous TiO_2, and commercial TiO_2 (ST-01, P-25, JRC-01, and JRC-03). The solar energy conversion efficiency of the cell using nanorods/nanoparticles TiO_2 with mesoporous structure was about 7.12% while η of the cell using P-25 reached 5.82%. These materials are promising for chemical and energy-related applications such as photocatalytic activity materials, a semiconductor in dye-sensitized solar cell.

Acknowledgements

The authors would like to express gratitude to Prof. S. Isoda and Prof. H. Kurata, Institute for Chemical Research, Kyoto University for the use of TEM apparatus Prof. T. Yoko, Institute for Chemical Research, Kyoto University for the use of XRD equipment. Prof. Mochizuki at AIST for the kind supply of Pt counter electrode. We are also grateful to the Geomatec Co. Ltd. for providing a part of conducting glass. This work was supported by grant-in-aids from the Ministry of Education, Science Sports, and Culture of Japan under the 21 COE program, the Nanotechnology Support Project, and from NEDO under high-performance dye-sensitized solar cell project, and from JSPS research fellow. We acknowledge the anonymous reviewers for the helpful discussion to improve the manuscript.

References

[1] C.N.R. Rao, M. Nath, Dalton Trans. 1 (2003) 1.
[2] G.R. Patzke, F. Krumeich, R. Nesper, Angew. Chem. Int. Ed. 41 (2002) 2446.
[3] M. Huang, S. Mao, H. Feick, H. Yan, Y. Wu, H. Kind, E. Weber, R. Russo, P. Yang, Science 292 (2001) 1897.
[4] Z.W. Pan, Z.R. Dai, Z.L. Wang, Science 291 (2001) 1947.
[5] L. Miao, S. Tanemura, S. Toh, K. Kaneko, M. Tanemura, Appl. Surf. Sci. 238 (2004) 175.
[6] C. Xu, Y. Zhan, K. Hong, G. Wang, Solid State Commun. 126 (2003) 545.
[7] B. Cheng, J.M. Russell, W. Shi, L. Zhang, E.T. Samulski, J. Am. Chem. Soc. 126 (2004) 5972.
[8] S. Pavasupree, Y. Suzuki, A. Kitiyanan, S. Pivsa-Art, S. Yoshikawa, J. Solid State Chem. 178 (2005) 2152.
[9] S. Pavasupree, Y. Suzuki, S. Pivsa-Art, S. Yoshikawa, Sci. Tech. Adv. Mater. 6 (2005) 224.
[10] A. Fujishima, T.N. Rao, D.A. Tryk, J. Photochem. Photobiol. C: Photochem. Rev. 1 (2000) 1.
[11] M. Adachi, Y. Murata, M. Harada, S. Yoshikawa, Chem. Lett. 8 (2000) 942.
[12] M. Adachi, I. Okada, S. Ngamsinlapasathian, Y. Murata, S. Yoshikawa, Electrochemistry 70 (2002) 449.
[13] M. Adachi, Y. Murata, I. Okada, S. Yoshikawa, J. Electrochem. Soc. 150 (8) (2003) G488.
[14] S. Ngamsinlapasathian, T. Sreethawong, Y. Suzuki, S. Yoshikawa, Sol. Energy Mater. Sol. Cells 86 (2005) 269.
[15] S. Pavasupree, Y. Suzuki, S. Pivsa-Art, S. Yoshikawa, Ceram. Int. 31 (2005) 959.
[16] S. Pavasupree, Y. Suzuki, S. Pivsa-Art, S. Yoshikawa, J. Solid State Chem. 178 (2005) 128.
[17] T. Sreethawong, Y. Suzuki, S. Yoshikawa, J. Solid State Chem. 178 (2005) 329.
[18] A. Kitiyanan, S. Ngamsinlapasathian, S. Pavasupree, S. Yoshikawa, J. Solid State Chem. 178 (2005) 1044.
[19] S. Sakulkhaemaruethai, S. Pavasupree, Y. Suzuki, S. Yoshikawa, Mater. Lett. 59 (2005) 2965.
[20] Y. Suzuki, S. Pavasupree, S. Yoshikawa, R. Kawahata, J. Mater. Res. 20 (2005) 1063.
[21] S. Pavasupree, Y. Suzuki, S. Yoshikawa, R. Kawahata, J. Solid State Chem. 178 (2005) 3110.
[22] Y. Suzuki, S. Ngamsinlapasathian, R. Yoshida, S. Yoshikawa, Central Eur. J. Chem., in press.
[23] Y. Suzuki, S. Yoshikawa, J. Mater. Res. 19 (2004) 982.
[24] R. Yoshida, Y. Suzuki, S. Yoshikawa, Mater. Chem. Phys. 91 (2005) 409.
[25] R. Yoshida, Y. Suzuki, S. Yoshikawa, J. Solid State Chem. 178 (2005) 2179.
[26] S. Uchida, R. Chiba, M. Tomiha, N. Masaki, M. Shirai, Electrochemistry 70 (2002) 418.
[27] J.-H. Yoon, S.-R. Jang, R. Vittal, J. Lee, K.-J. Kim, J. Photochem. Photobiol. A: Chem. 186 (2006) 184.